Received: 29 October 2018 | Revised: 26 September 2019 | Accepted: 10 November 2019 | Published on: 23 December 2019

DOI: 10.1002/met.1863

RESEARCH ARTICLE

Meteorological Applications RMetS

Climate change effect on water resources in Varanasi district, India

Mărgărit-Mircea Nistor[1,2] | Praveen K. Rai[3,4] | Vikas Dugesar[4] | Varun N. Mishra[5,6] | Prafull Singh[3] | Aman Arora[7] | Virendra Kumar Kumra[4] | Iulius-Andrei Carebia[8]

[1]Romanian Academy, National Institute for Economic Research "Costin C. Kiritescu" of the Romanian Academy/ Centre for Mountain Economy (CE-MONT), Vatra Dornei, Romania

[2]Department of Hydrogeology, Earthresearch Company, Cluj-Napoca, Romania

[3]Amity Institute of Geo-Informatics and Remote Sensing, Amity University, Noida, India

[4]Department of Geography, Institute of Science, Banaras Hindu University, Varanasi, India

[5]Centre for Climate Change and Water Research, Suresh Gyan Vihar University, Jaipur, India

[6]Department of Physics, Indian Institute of Technology (BHU), Varanasi, India

[7]Department of Geography, Faculty of Natural Sciences, JMI University, New Delhi, India

[8]Department of Educational Technology, German European School, Singapore, Singapore

Correspondence
Mărgărit-Mircea Nistor, Department of Hydrogeology, Earthresearch Company, Cluj-Napoca, 400667, Romania.
Email: renddel@yahoo.com

Abstract

Evapotranspiration and water availability are driven by changing climate and land cover parameters. In the present study, climatological records and land cover data were analysed simultaneously to accomplish the spatial distributions of climate change effects on water resources in Varanasi district, north India. Humidity–aridity was assessed by Lang's rain factor and De Martonne's aridity index, based on mean monthly rainfall and air temperature from seven meteorological stations. The climate change effect on water resources was evaluated using a 5 × 5 matrix that includes water availability and the aridity index by considering two time periods: 1941–1970 (1950s) and 1971–2000 (1980s). The methodology is based on seasonal crop evapotranspiration (ET_c) (initial, mid-season, end season and cold season) and annual water availability calculations. The high values (≤ 1,045 mm) of ET_c were identified during the mid-season stage. Water availability indicates decreases in the maximums from 718 to 636 mm during the two analysed periods, with a negative impact at the spatial scale. Lang's rain factor (< 40) indicates an arid climate in the northwest, west, east and central parts of the district and a humid climate (Lang's rain factor > 40) in the south. De Martonne's aridity index indicates rapid aridization from south to north (28.3 in the 1950s and 25.6 in the 1980s). The high and very high climate effects on water resources in Varanasi district were found mainly in the crop lands, while in the urban areas the climate effect is low. The much affected area by climate change and land cover was depicted during the recent period (1980s). This statement was proved also by the Mann and Kendall test, which indicates a negative trend for annual precipitation at all stations (for the period 1941–2000), while the mean annual temperature had a positive trend for four stations. These findings suggest that climate change had a negative effect on water resources during the last 60 years in the study area.

KEYWORDS

climate change, climate indices, evapotranspiration, land cover, Varanasi district, water resources

1 | INTRODUCTION

Climatic variables are in continuous change due to variation in global systems and could have a major impact on water resources at the regional scale. Climate and land cover are two components of the Earth's system, which changes to a greater degree. Changes in vegetation and land-use patterns for urbanization and agricultural practices contribute to the change in the water resources quality–quantity status. In addition, the Industrial Revolution in the latter half of the 18th century led to unprecedented changes in land-use patterns and influence the climate around the world (Meinshausen *et al*., 2009). Last century witnessed a substantial change in global mean temperature and sea level. From the late 20th century, every passing decade has been warmer than the preceding one (Frich *et al*., 2002; Quirk, 2012); the last five decades are the successively hottest decades in 1,400 years of climate events' recorded history.

At present, the warming climate is leading towards less mean precipitation and higher mean temperatures. Many of the worldwide debates are addressing the spatio-temporal impacts (Chattopadhyay and Hulme, 1997; Parry *et al*., 2004) of global warming on climatic variables and dependent ecosystems. Various climatic and hydrological parameters, rainfall, relative humidity, sunshine and evapotranspiration are expected to face the unpleasant consequences of climate change. According to Shaver *et al*. (2000), owing to the changing climate, the Earth is changing its weather conditions. In consequence, the regional climatic conditions are also changed mainly for rainfall and temperature (Shan *et al*., 2015). Different regions of the world show differential responses to global climate change. The changes in temperature and rainfall patterns, combined with other complex anthropological factors, govern the regional and local hydrological variables (Prăvălie, 2014; Prăvălie *et al*., 2014; Nistor *et al*., 2018). Reduced precipitation coupled with high temperatures could have a negative impact on surface waters and groundwater (Loáiciga *et al*., 2000; Bachu and Adams, 2003; Brouyère *et al*., 2004; Nistor, 2019).

Various studies have been conducted regarding the impacts of precipitation, potential evapotranspiration (ET_0) and actual evapotranspiration (AET_0) on ecosystems and the regional water balance (Allen, 2000; Gerrits *et al*., 2009; Cheval *et al*., 2011; Prăvălie *et al*., 2014). Many of them argued about AET_0 and its use as an indicator for climate change and water balance. Worldwide, the ET_0 over Taiwan (Yu *et al*., 2002), in various areas of Iran (Tabari *et al*., 2011) and parts of the Mediterranean (Espadafor *et al*., 2011; Palumbo *et al*., 2011) show an increasing trend in the last couple of decades. Papaioannou *et al*. (2011) reported a decreasing trend of annual ET_0 between 1950 and 1980 in Greece, but it reverses after 1980 and continues increasing after that point. Similarly, ET_0 decreased abruptly during the 1990s in the Wei River area of China and it has continued to increase further ever since (Zuo *et al*., 2012).

In the South Asia, the climatic characteristics of the rainfall regime are heterogeneous. Thus, rainfall variability indicates a declining trend of rainfall with a more regular deficit monsoon (Watson, 2001; IPCC, 2013; Jiménez Cisneros *et al*., 2014). The regional differences in climate change impacts and warming trends in continental interiors are strongest in Asia. Rainfall increased in the last century over Northern and Central Asia and decreased over Southern Asia. Mean seasonal rainfall in South Asia are declining perceptibly with the regular occurrence of monsoon deficient seasons under spatial irregularities. Over India, and in some regions of South Asia, the number of heavy rainfall events is increasing at the expense of decreasing low-intensity rainfall events (Jiménez Cisneros *et al*., 2014).

In addition to climate change, human water demand represents in various locations reasons for the water crisis (Wang and Dickinson, 2012; Fu *et al*., 2014). The change in water availability under climate change signals the necessity for adaptation. In Varanasi district and in the entire Uttar Pradesh state region, along with rapid economic development and population growth, water withdrawals from the main rivers' basins (i.e. Ganga, Yamuna, Ghaghra) have increased significantly. Various studies have examined the changes in water supply under climate change, but few have considered the joint pressures from climate change, land cover and socioeconomic development. It becomes indispensable to develop a quantitative approach to evaluate future water scarcity in a changing environment at the regional scale.

The importance of a crop evapotranspiration (ET_c) study is closely related to hydrological characteristics. Thus, the water balance, water availability and effective precipitation variation at the spatial scale over the long term contribute to the evaluation of surface water discharge oscillations and an assessment of groundwater recharge. This kind of study has a high relevance on groundwater, agriculture and the future management of natural resources both for Varanasi district and for similar territories in South Asia.

The main objective of the present study is to assess the climate change effect on water resources in Varanasi district using climate and land cover data. Lang's rain factor, De Martonne's aridity index and water availability were considered for spatio-temporal-scale analysis. The applied method is based on an inference 5 × 5 matrix, which combines the aridity index with water availability during the 1950s and 1980s to evaluate the climate effect on water resources in these two time shifts. The approach and analysis at the spatial scale were performed in an ArcGIS environment.

2 | STUDY AREA

Varanasi, also known as Kasi or Banaras, is the religious, cultural and educational capital of India. Varanasi district is located in the middle Gangetic plain of the western part of Uttar Pradesh (Figure 1). Its geospatial boundaries spread between 82°39′ and 83°11′ E longitude and between 25°10′ and 25°34′ N latitude. The geographical area is 1,535 km^2; the total population is 3,676,841, with a density of 2,395 individuals·km^{-2}. In the study area, about 43.44% of the population lives in the urban area, while about 56.56% lives rurally.

The study area is mainly part of the Ganga, Varuna and Gomati rivers (Rai and Mohan, 2014; Rai and Nathawat, 2017). The media of groundwater is mainly composed of sedimentary deposits. The favourable life conditions such as fertile soil, a plain topography and water availability make it able to bear a high population density (Rai and Nathawat, 2017).

According to the Koppen Climate Classification, Varanasi district has a humid subtropical climate (Cwa or Cwb) class (Kottek *et al.*, 2006). These climate types are characterized by dry winters with main temperatures that vary between 3 and 18°C; summers mainly have a constant rainfall and mean temperatures > 22°C.

3 | MATERIALS AND METHODS

3.1 | Climate data

In the present study, a mean monthly air temperature from 1941 to 2000 is used to calculate the ET_0. The precipitation data from the same period were used to carry out the AET_0 and water availability. The climate data were collected from seven meteorological stations located in Varanasi district and its surroundings. The source of the climate data is the Indian Meteorological Department (IMD) in Pune (http://www.imdpune.gov.in/). These climatic stations are well distributed spatially, which can show the general characteristics of the regional climate. The temperature and precipitation data were homogenized and corrected for the long-term period before being used in the study. The average data sets of the periods 1941–1970 (1950s) and 1971–2000 (1980s) were used in order to compared and perceive any possible oscillations in the climate variables and water availability. The term "water resources" here refers to surface waters and groundwater.

3.2 | Land cover data

Land cover data belong the Oak Ridge National Laboratory (ORNL) Distributed Active Archive Center (DAAC)

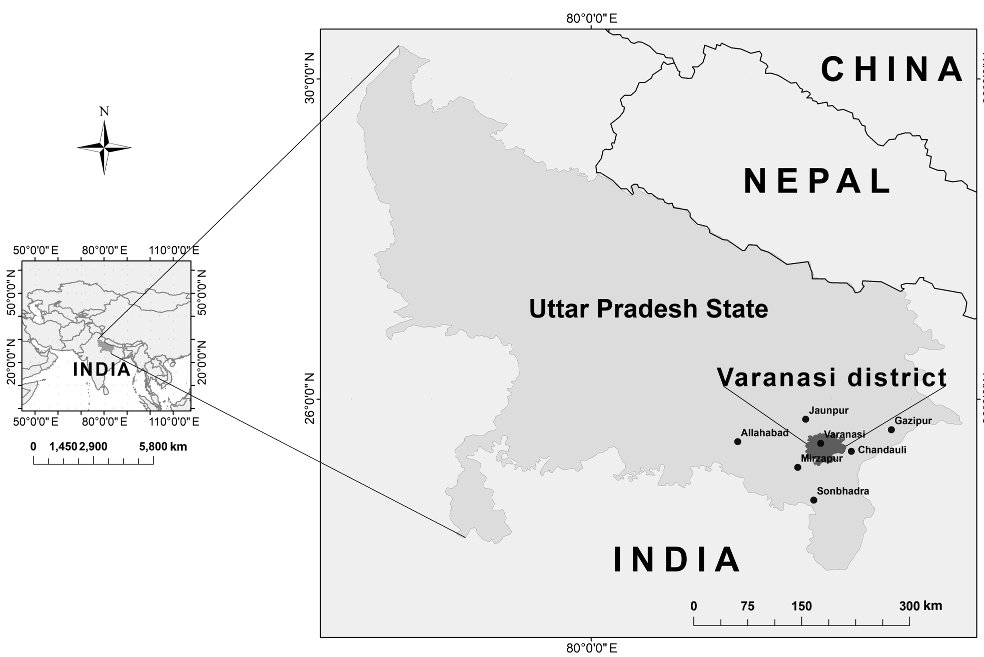

FIGURE 1 Location of Varanasi district (India) in Western Asia

and represent Decadal Land Use and Land Cover Classifications across India. This data set comprises eight classes which are classified as *per* the International Geosphere–Biosphere Programme (IGBP) classification scheme (Supporting Information Figure S1). Landsat data for 1985 and 2005 were used for land cover extraction of Varanasi district. These temporal data were classified through a supervised classification method to prepare land cover of the area.

The spatial resolution was set at 100 m resolution (Roy *et al.*, 2015). The study area is then extracted and processed in an ArcGIS environment.

3.3 | Mann and Kendall test

Climate parameters of annual precipitation and mean annual temperature used in the present study were analysed separately for each station in order to understand the variables' trend over the period 1941–2000. The data were homogeneously controlled and verified and then inserted into the Mann and Kendall (1975) test. This is a non-parametric test that focuses on the assessment of statistical significance of the different trends. It is widely used in climatology and hydrology because it performs on the time-series data values (Gilbert, 1987; Hamed, 2008; Cervi and Nistor, 2018). For the S-value equivalent to zero, the Mann and Kendall test indicates no trend in the respective series. The test assesses the time series considering if more recent data are greater that the oldest ones. In this case, the S-value is incremented showing a positive trend. Inversely, in case the recent data value is lower than the oldest, the S-values will decrease, and the negative trend is called.

Equation (1) expresses the Mann and Kendall statistic (S) formula:

$$S=\sum_{k=1}^{n-1}\sum_{j=k+1}^{n} sign\left(x_j-x_k\right) \tag{1}$$

where

$sign(x_j - x_k) = 1$ if $x_j - x_k > 0$

$sign(x_j - x_k) = 0$ if $x_j - x_k = 0$

$sign(x_j - x_k) = -1$ if $x_j - x_k < 0$.

The test follows two hypotheses: the zero hypothesis that indicates the absence of the trend in the time series; and the alternative hypothesis in which there is a statistically relevant trend in the time series for the given relevance level (α). The p-value has a central role in the Mann and Kendall test. The p-value determines the hypothesis reliability level. If the p-value is smaller than the selected α relevance level (commonly $\alpha = 0.05$ or 5%). Oppositely, if p is larger than the α relevance level, then the hypothesis is adopted.

3.4 | Evapotranspiration and water availability

3.4.1 | Potential evapotranspiration (ET_0)

The ET_0 for Varanasi district during the period 1941–2000 was calculated using mean monthly air temperature data by the Thornthwaite (1948) method (Equation 2). This method is very valuable at the regional scale, not only in climatological matters but also in hydrogeological and agricultural studies, for a long-term period (Zhao *et al.*, 2013; Čenčur Curk *et al.*, 2014; Cheval *et al.*, 2017). Dezsi *et al.* (2018) have used the Thornthwaite method in a study on evapotranspiration and water availability in Europe. Further, the ET_0 is multiplied by a crop co-efficient (K_c) to find the crop evapotranspiration (ET_c):

$$ET_0=16bi\left(\frac{10T_i}{I}\right)^{\alpha}\ (\mathrm{mm\cdot month-1}) \tag{2}$$

where ET_0 is the potential evapotranspiration; bi is the radiation parameter for specific latitude (Table 1); T_i is the monthly air temperature; I is the annual heat index (Equation 3); and α is the complex function of heat index (Equation 4):

$$I=\sum_{i=1}^{12}\left(\frac{T_i}{5}\right)^{1.514} \tag{3}$$

$$\alpha=6.75\times10^{-7}I^3-7.71\times10^{-5}I^2+1.7912\times10^{-2}I+0.49239 \tag{4}$$

3.4.2 | Seasonal and annual crop evapotranspiration (ET_c)

In general, the K_c is used to calculate the ET_c by multiplying the former by ET_0. The

K_c is representative for different climatic zones; hence, it differs with the place and crop types in the area. At the same time, the K_c varies with the growth stages, even for the same crop either in the same area or in a different area. Crop growth period shows distinct K_c values due to a change in land cover and vegetation type (Allen *et al.*, 1998; Grimmond and Oke, 1999). Therefore, four developmental stages of crop growth in one year were used in the present study. A specific K_c was assigned to each land cover type for four seasons. This approach is useful to calculate the ET_c for long-term period.

TABLE 1 Sunshine parameter (units of 30 days of 12 hr)

Month	January	February	March	April	May	June	July	August	September	October	November	December
bi (25° N latitude)	0.93	0.89	1.03	1.06	1.15	1.14	1.17	1.12	1.02	0.99	0.91	0.91

Source: Thornthwaite (1948).

The values of K_c are different at successive stages of crop growth as follows: initial season (March–May), mid-season (June–August), end of season (September–November) and cold season (December–February). Therefore, a particular K_c was used for every season: the $K_{c\ ini}$ for the initial season, the $K_{c\ mid}$ for the mid-season, the $K_{c\ end}$ for the end season and the $K_{c\ cold}$ for the cold season (Supporting Information Figure S2). The evapotranspiration rate for bare soil and the urban areas of the United States was first reported by Grimmond and Oke (1999). Land cover classes and representative seasonal K_c co-efficients for Varanasi district are illustrated in Table 2. Based on monthly ET_0 and K_c values, the seasonal ET_c was calculated for the four stages: $ET_{c\ ini}$ (Equation 5), $ET_{c\ mid}$ (Equation 6), $ET_{c\ end}$ (Equation 7) and $ET_{c\ cold}$ (Equation 8). The annual ET_c was then calculated by summing all four seasonal ET_c (Equation 9):

$$ET_{c\,ini} = ET_{0\,ini} \times K_{c\,ini} \tag{5}$$

$$ET_{c\,mid} = ET_{0\,mid} \times K_{c\,mid} \tag{6}$$

$$ET_{c\,end} = ET_{0\,end} \times K_{c\,end} \tag{7}$$

$$ET_{c\,cold} = ET_{0\,cold} \times K_{c\,cold} \tag{8}$$

$$\text{Annual}\,ET_c = ET_{c\,ini} + ET_{c\,mid} + ET_{c\,late} + ET_{c\,cold} \tag{9}$$

3.4.3 | Actual crop evapotranspiration (AET_c)

The Budyko approach (Equation 10) (Budyko, 1974) was used to calculate the AET_c using the annual ET_c and precipitation data. Through Budyko's formula, the water balance could be determined and this approach is significant to know if the heat energy is enough to produce the evaporation from the precipitation data (Gerrits *et al.*, 2009; Čenčur Curk *et al.*, 2014). The vegetation evapotranspiration was considered in the AET_c calculation by including ET_c in the formula of aridity index (Equation 11).

$$\frac{AETc}{PP} = \left[\left(\varphi tan\frac{1}{\varphi}\right)\left(1 - exp^{-\varphi}\right)\right]^{0.5} \tag{10}$$

where AET_c is the actual land cover evapotranspiration (mm); PP is the total annual precipitation (mm); and φ is the aridity index (Equation 11):

TABLE 2 Land cover classes and representative seasonal K_c co-efficients for Varanasi district

Land cover description	$K_{c\ ini}$ season					$K_{c\ mid}$ season					$K_{c\ end}$ season					$K_{c\ cold}$ season				
	K_c	K_s	K_u	K_w	K_{clc}	K_c	K_s	K_u	K_w	K_{clc}	K_c	K_s	K_u	K_w	K_{clc}	K_c	K_s	K_u	K_w	K_{clc}
Built-up land	–	–	0.20	–	0.20	–	–	0.40	–	0.40	–	–	0.25	–	0.25	–	–	–	–	–
Wasteland	–	–	0.16	–	0.16	–	–	0.36	–	0.36	–	–	0.26	–	0.26	–	–	–	–	–
Plantation	0.30	–	–	–	0.30	1.05	–	–	–	1.05	0.50	–	–	–	0.50	–	–	–	–	–
Cropland	1.10	–	–	–	1.10	1.35	–	–	–	1.35	1.25	–	–	–	1.25	–	–	–	–	–
Shrubland	0.80	–	–	–	0.80	1	–	–	–	1	0.95	–	–	–	0.95	–	–	–	–	–
Fallow land	0.40	–	–	–	0.40	0.60	–	–	–	0.60	0.50	–	–	–	0.50	–	–	–	–	–
Permanent wetlands	–	–	–	0.15	0.15	–	–	–	0.45	0.45	–	–	–	0.80	0.80	–	–	–	–	–
Water bodies	–	–	–	0.25	0.25	–	–	–	0.65	0.65	–	–	–	1.25	1.25	–	–	–	–	–

Note: K_c: crop co-efficient for plants; K_s: evaporation co-efficient for bare soils; K_u: crop co-efficient for urban areas; K_w: evaporation co-efficient for open water; K_{clc}: crop co-efficient for land cover.
Sources: Allen *et al.* (1998); Nistor and Porumb-Ghiurco (2015); Nistor (2019).

$$\varphi = \frac{ETc}{PP} \tag{11}$$

3.4.4 | Water availability

Water availability was determined for the 1950s and 1980s from the difference in the annual precipitation and the AET_c calculated for the same subperiods. The infiltration process for a long-term period could be neglected (Čenčur Curk *et al.*, 2014) considering that the infiltration is a transitional function of permeability. The mathematical calculations at the spatial scale (1 km^2 resolution) for the annual and seasonal ET_c, as well as water availability (Equation 12), were performed using the Raster Calculator function available in Spatial Analyst Tools from the ArcGIS environment.

$$\text{Water availability (mm)} = \text{annual precipitation (mm)} - \text{annual AETc (mm)} \tag{12}$$

3.5 | Climate indices

3.5.1 | Lang's rain factor

Lang (1915) could be considered the first scientist to propose the formula (Equation 13) for humidity–aridity in the base of precipitation and temperature data (Moreau, 1938). The concept of Lang's rain factor is based on the rise in temperature that influences the water deficit and makes soil sufficiently recharged by precipitation (Quan *et al.*, 2013):

$$I_{DM} = \frac{PP}{T} \tag{13}$$

where PP is the annual mean precipitation (mm); and T is the annual mean air temperature (°C).

3.5.2 | De Martonne's aridity index

In order to characterize the climate of the area and to determine the "humidity–aridity" at the regional scale, De Martonne's aridity index (Deniz *et al.*, 2011) was used (Equation 14). The method was proposed by De Martonne (1925, 1926) and is widely used for climatological, agricultural and hydrological studies (Zambakas, 1992):

$$I_{DM} = \frac{PP}{T + 10} \tag{14}$$

Table 3 reports the climate types according to De Martonne's (1925) and Lang's (1915) classifications.

3.6 | Matrix method for assessing the climate effect on water resources

De Martonne's aridity index indicates more classes for climate classification, and for this reason it was chosen to be used in the inference matrix together with the water availability parameter. The inference matrix is an approach used at the regional scale to evaluate the climate change effects on water resources (Nistor *et al.*, 2016). For spatial scale determination, Nistor and Mîndrescu (2019) bring forward an advance procedure that combines the two parameters into the ArcGIS using raster grid data. Practically, the approach is based on five classes of climate effect that resulted through a 5 × 5 matrix. The matrix is constructed from the classes of De Martonne's aridity index and classes of water availability, returning the effect classes as following: very low, low, medium, high and very high (Figure 2).

The classification of De Martonne's aridity index was set accordingly to standard classes of this index from extremely humid to Mediterranean class, while water availability was classified following Nistor and Mîndrescu's (2019) classes. The general frame of the applied methodology is illustrated in Figure 3.

TABLE 3 Climatic classification

Lang's rain factor		
Climate types	**Classes**	
Per-humid	> 160	
Humid	40–160	
Arid	< 40	
De Martonne's aridity index (IDM)		
Climate types	**Classes**	**Precipitation (P) (mm)**
Extremely humid	> 55	$P > 800$
Very humid	35 ≤ IDM ≤ 55	$700 \leq P \leq 800$
Humid	28 ≤ IDM < 35	$600 \leq P \leq 700$
Semi-humid	24 ≤ IDM < 28	$50 \leq P < 600$
Mediterranean	20 ≤ IDM < 24	$400 \leq P < 500$
Semi-dry	10 ≤ IDM < 20	$200 \leq P < 400$
Dry	<10	$P < 200$

4 | RESULTS

4.1 | Variation of climate and annual trends of PP and TT over the period 1941–2000

The climate of Varanasi district between 1941 and 2000 indicates a mean annual temperature at around 25°C. Thus, during the 1950s, the mean annual temperature varied between 25.29 and 25.89°C (Supporting Information Figure S3a), and during the 1980s it varied between 25.22 and 25.76°C (Figure S3b). The annual precipitation was between 1,014 and 1,135 mm (1950s) and between 914 and 1,042 mm (1980s) (Figure S3c,d). During the 1950s, the annual ET_0 varied between 1800 and 1988 mm (Figure S3e), and during the 1980s it varied between 1,765 and 1923 mm (Figure S3f). The shifting in the ET_0 values between the two periods is more related to temperature increases in the respective areas.

Overall, the climate variation over the period 1941–2000 would likely indicate a slight decrease in mean annual temperature (about 0.1°C) and annual ET_0 (about 65 mm). Precipitation decreased between the 1950s and the 1980s by about 100 mm, a fact that means the study of evapotranspiration and water availability for water resources is very important. These changes have a negative influence on the water resources on the long term in Varanasi district.

During the period 1941–2000, the Mann and Kendall test indicates a negative trend ($S < 0$) in annual precipitation for all analysed stations (alpha = 0.5) (Table 4). This aspect is also shown in Figure 4a,c,e,g,i,k,m, where all stations were found with a negative trend for annual precipitation. For all stations, it was found that the negative precipitation trend is non-significant ($p < 0.1$).

According to the Mann and Kendall test, the mean annual temperature has a positive trend ($S > 0$) for four stations (Chandouli, Gazipur, Mirzapur and Sonbhadra) and a negative trend ($S < 0$) for three stations (Allahabad, Jaunpur and Varanasi) (Table 5). For the mean annual temperature, the test indicates significant trends ($p > 0.1$). Figure 4b,d,f,h,j,l,n illustrate the annual variation of mean temperatures. Gazipur Station has a slightly negative trend, which is contrary to the Mann and Kendall test results ($S = 14$). However, Allahabad and Jaunpur stations are located out of Varanasi district, much in the interior of the continent, and for this reason

Climate type	De Martonne Index	Effect	Water availability (mm)				
			0 - 100	101 - 200	201 - 400	401 - 600	> 600
		Effect	Very high	High	Medium	Low	Very low
Extremely humid	> 55	Very low	Medium	Low	Low	Very low	Very low
Very humid	35 ≤ IDM ≤ 55	Low	High	Medium	Low	Low	Very low
Humid	28 ≤ IDM < 35	Medium	High	High	Medium	Low	Low
Semi-humid	24 ≤ IDM < 28	High	Very high	High	High	Medium	Low
Mediterranean	20 ≤ IDM < 24	Very high	Very high	Very high	High	High	Medium

Climate change effect				
Very high	High	Medium	Low	Very low

FIGURE 2 Inference matrix used to assess the climate effect on the water resources of Varanasi district

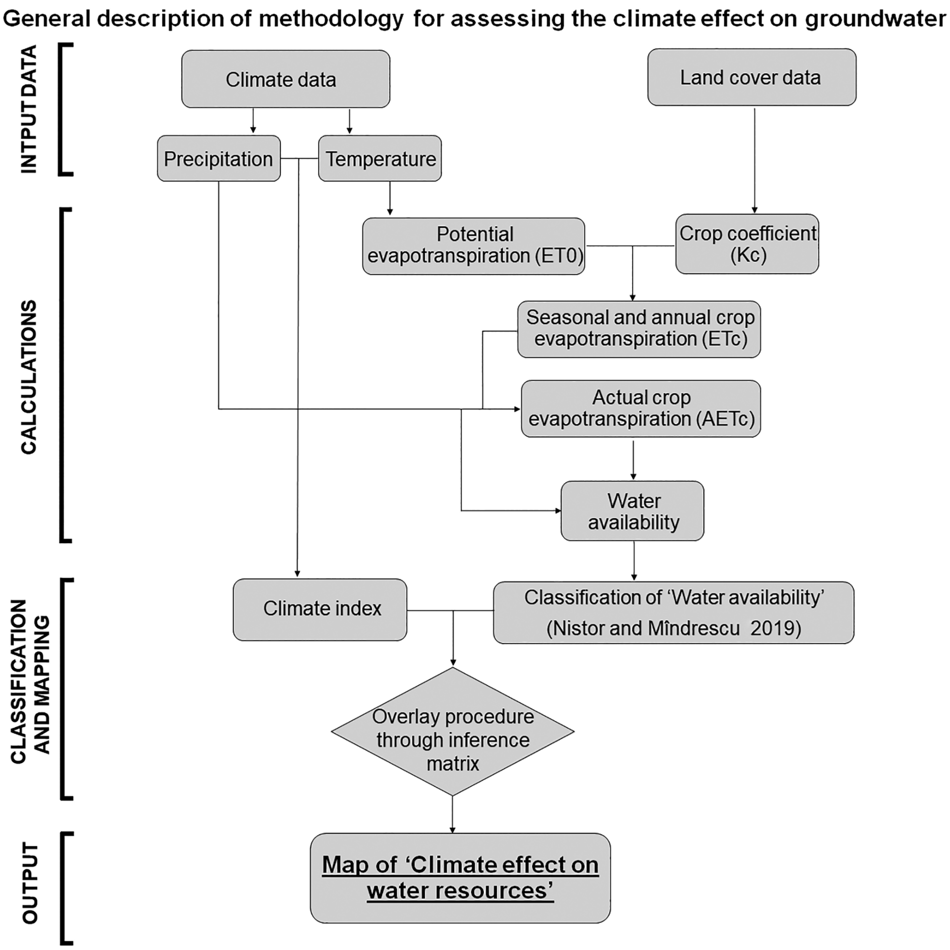

FIGURE 3 Schematic diagram illustrating the methodological procedure

the mean annual temperature trend could be negative, while Varanasi Station has a *S*-value slightly < 0.

4.2 | Variation of evapotranspiration

Seasonal and annual ET_c were determined for Varanasi district including the vegetation layers. During the 1950s, the seasonal ET_c shows up to 805 mm for the $ET_{c\ ini}$ and up to 766 mm for the $ET_{c\ ini}$ related to the 1980s. The $ET_{c\ mid}$ recorded the highest values of the seasonal ET_c in both periods. Thus, the $ET_{c\ mid}$ varied from 259 to 1,099 mm during the 1950s, while in the 1980s the $ET_{c\ mid}$ varied from 251 to 1,045 mm. At the end of the season, the $ET_{c\ end}$ indicate values from 83 to 449 mm (1950s) and from 86 to 463 mm (1980s). For all three seasons, the maximums of the ET_c were found in the north of the district, while the minimums were in the

TABLE 4 Mann–Kendall trend test statistic applied for annual precipitation

Test/station	Chandouli	Allahabad	Jaunpur	Gazipur	Mirzapur	Sonbhadra	Varanasi
Kendall's tau	−0.25	−0.20	−0.25	−0.35	−0.21	−0.22	−0.24
S	−436.00	−355.00	−438.00	−620.00	−374.00	−390.00	−430.00
Var(*S*)	24,583.33	24,582.33	24,583.33	24,583.33	24,583.33	24,583.33	24,583.33
p-value (two-tailed)	0.01	0.02	0.01	< 0.0001	0.02	0.01	0.01
Alpha	0.05	0.05	0.05	0.05	0.05	0.05	0.05

southeast, mainly in the artificial and water bodies areas. Supporting Information Figure S4 shows the spatial distribution of the seasonal ET_c in Varanasi district.

The annual ET_c varied from 452 to 2,352 mm (1950s) and from 444 to 2,265 mm (1980s). The decreasing evapotranspiration in both seasonal and annual between the two periods is due to the slightly decreasing mean monthly and annual temperatures. The cropland of the district resulted in a high evapotranspiration rate (> 2000 mm) in the annual ET_c in both periods. Figure 5a,b illustrates the spatial distribution of the annual ET_c in Varanasi district.

Interestingly, the annual AET_c indicates higher values (> 900 mm) in the south of Varanasi district, especially in the 1980s. This inversion between annual ET_c and annual AET_c at the spatial scale is highly correlated with the precipitation values. Thus, in the southern part of the district, the precipitation is higher than in the northern part and the AET_c has higher values in the south. On the contrary, owing to the lack of precipitation in the north, the AET_c records fewer values. For both analysed periods, the lower values of AET_c (around 400 mm) were depicted in the urban areas and wasteland. Figure 5c,d shows the spatial distribution of annual AET_c in the study area.

4.3 | Variation of water availability

The water availability in Varanasi district was determined based on the annual precipitation and annual AET_c during the 1950s and 1980s. During the first period (1950s), the water availability ranged from 81 to 718 mm, recording its higher values (> 700 mm) on the southeastern sides of the district and lower values (< 100 mm) on the northwestern side (Figure 6a). During the second period (1980s), the water availability ranged from 62 to 636 mm, indicating the higher values (> 600 mm) in the southeast with a few artificial areas, while the lower values (< 100 mm) were in the central, north, west and east parts of the district (Figure 6b).

The decreasing water availability in Varanasi district is related to decreasing precipitation during the 1980s. Moreover, the extended territory with lower water availability (< 100 mm) during the 1980s is larger than during the 1950s. This is a negative aspect coming from the climate change, both for temporal and spatial scales.

4.4 | Variation of climate indices

Lang's rain factor indicates an arid climate (1950s) with an index < 40 in the northwest of the region and a humid climate with a factor > 40 in the south, west, east and central parts (Figure 7a). The same factor indicates an arid climate (1980s) in the north, west, east and central parts, while a humid climate was identified in the south (Figure 7b).

The spatial distribution of De Martonne's aridity index in Varanasi district is shown in Figure 7c,d. During the 1950s, the index is between 28.3 and 32.2, denoting a humid climate. At a spatial scale, it is observed that the lower values (close to 28) are extending in the north and northwest parts of Varanasi district, while the higher values (> 32) are extending in the south. During the 1980s, De Martonne's aridity index is between 25.6 and 29.6, denoting sub-humid and humid climates. Thus, the northern, eastern, western and central parts are characterized by a sub-humid climate, while the southern part of the district is characterized by a humid climate. The decreasing De Martonne's aridity index between the 1950s and 1980s, but also the spatial distribution over Varanasi district, suggest that the humid climate class, for the most of the northern part, is switched to a sub-humid climate class. This detail indicates an aridization in the northern part of Varanasi district due to climate change.

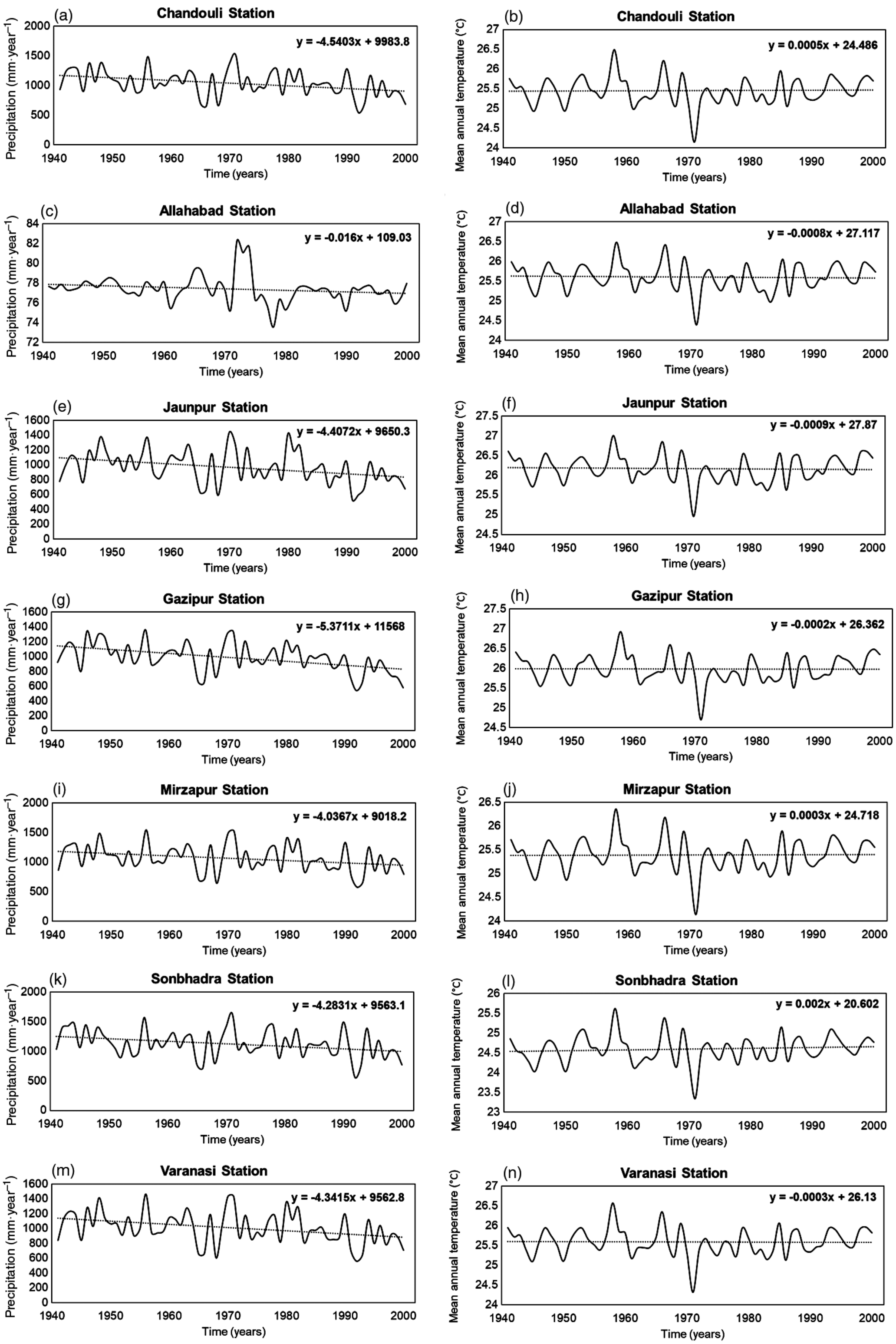

FIGURE 4 Annual trends of precipitation and temperature at meteorological stations during the period 1941–2000

4.5 | Climate change effect on water resources

Using a 5 × 5 matrix, the water availability was combined with De Martonne's aridity index to determine the climate change effects on water resources in Varanasi district. The 1950s experienced a high climate change effect in most of the territory, while the low and medium effects were depicted in the east and southeast parts, yet sparsely in the district. Interestingly, the very high impact

TABLE 5 Mann–Kendall trend test statistic applied for mean annual temperature

Test/station	Chandouli	Allahabad	Jaunpur	Gazipur	Mirzapur	Sonbhadra	Varanasi
Kendall's tau	0.02	−0.02	−0.03	0.01	0.02	0.10	0.00
S	42.00	−38.00	−48.00	14.00	42.00	172.00	−6.00
Var(*S*)	24,583.33	24,583.33	24,583.33	24,583.33	24,583.33	24,583.33	24,583.33
p-value (two-tailed)	0.79	0.81	0.76	0.93	0.79	0.28	0.97
Alpha	0.05	0.05	0.05	0.05	0.05	0.05	0.05

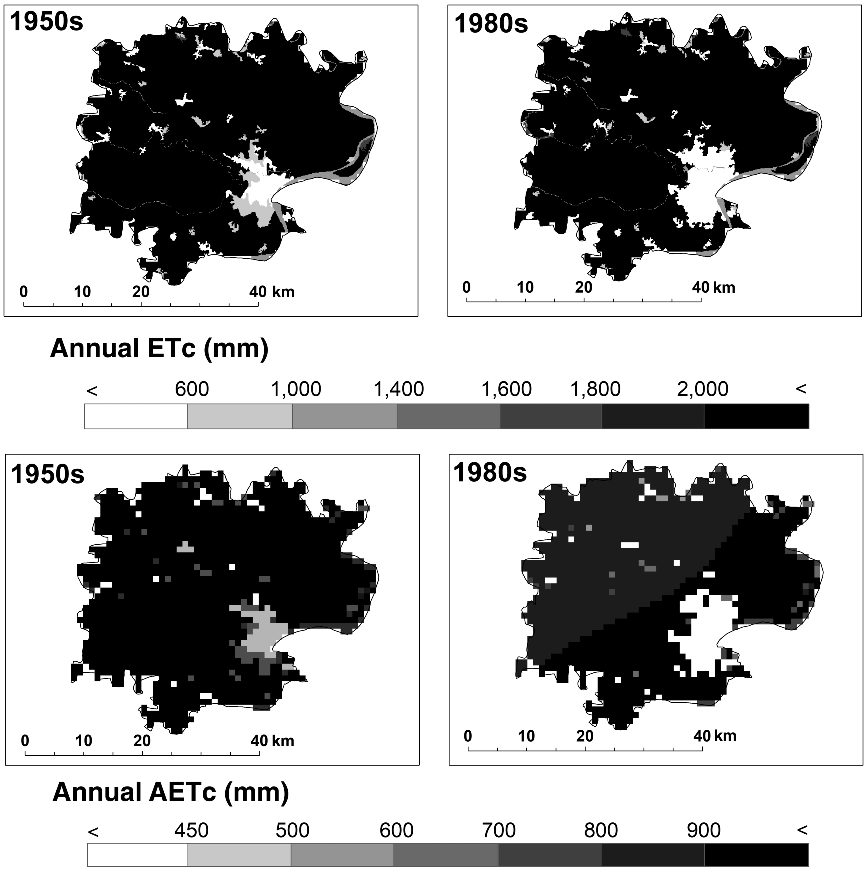

FIGURE 5 Spatial distribution of annual crop evapotranspiration (ET_c) and actual crop evapotranspiration (AET_c) in Varanasi district: (a) annual ET_c related to the 1950s; (b) annual ET_c related to the 1980s; (c) annual AET_c related to the 1950s; and (d) annual AET_c related to the 1980s

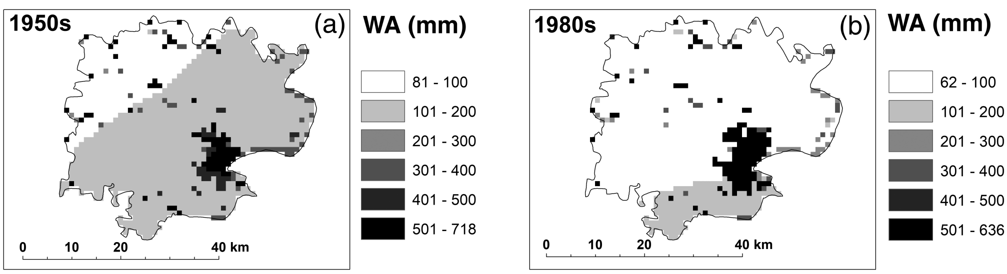

FIGURE 6 Spatial distribution of annual water availability (WA) in Varanasi district: (a) annual WA related to the 1950s; and (b) annual WA related to the 1980s

of climate change on water resources was not identified during the 1950s (Figure 8a).

During the 1980s, the climate change effect indicates a very high impact on water resources in the north, east, west and central parts of the district, while the high impact was depicted in the south. The medium climate change effect results much in the peripheral areas and sparsely in a few locations from the north and central sides. The low effect extends in the southeast sides and some locations from the south sides (Figure 8b). In both

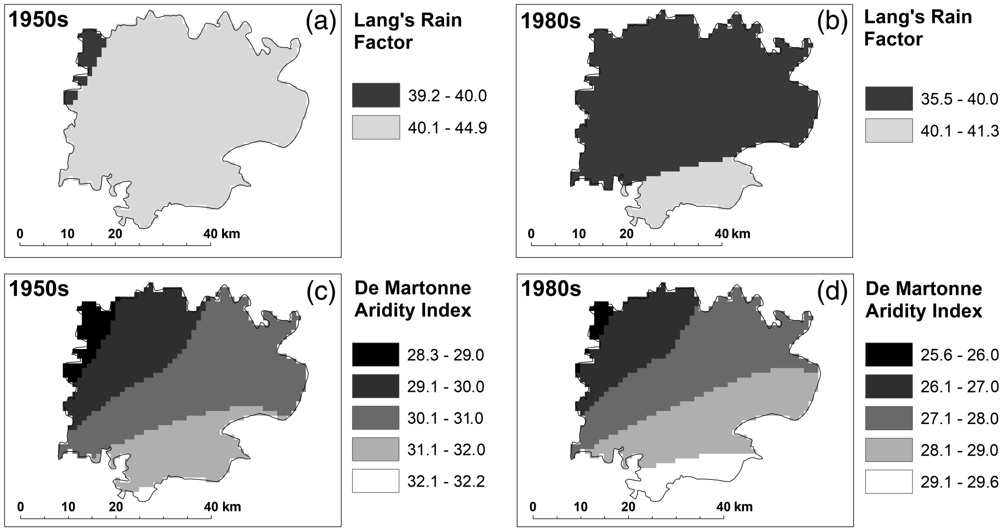

FIGURE 7 Spatial distribution of the Lang's rain factor and De Martonne's aridity index: (a) Lang's rain factor related to the 1950s; (b) Lang's rain factor related to the 1980s; (c) De Martonne's aridity index related to the 1950s; and (d) De Martonne's aridity index related to the 1980s

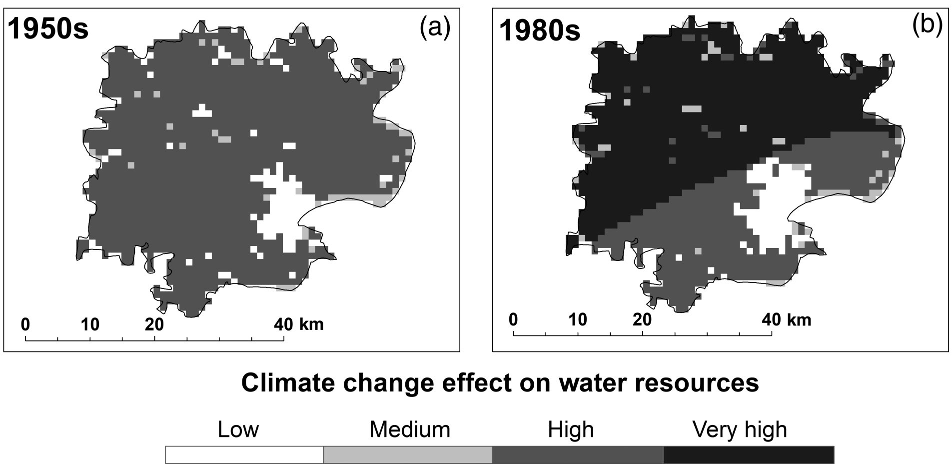

FIGURE 8 Climate effect assessment on water resources in Varanasi district: (a) spatial distribution of climate effect during the 1950s; and (b) spatial distribution of climate effect during the 1980s

periods, the high and very high effects are located in the cultivated areas and in the lands where the water availability is lower.

The analysis carried out through the water availability and De Martonne's aridity index in Varanasi district indicates a negative impact of the climate change effect on water resources. In addition, the decreasing precipitation and aridity index would suggest a higher effect on water resources and the possibility of depletion in the surface and groundwater quantity status: rivers' flow reduction, a declining in groundwater table and springs' discharge.

5 | DISCUSSION

The main goal of the present paper was to assess the climate change effect on water resources in the Varanasi district of India. An analysis of the 60 year climate data was completed by evapotranspiration and water availability calculations. In addition, the survey included the land cover and De Martonne's aridity index parameters. The evaluation of the climate change effect during the long term was completed through a 5 × 5 inference matrix by combining water availability and De Martonne's aridity index. The effect of climate change on water resources is divided into five impact classes following the standard procedure proposed by Nistor *et al.* (2016) and Nistor and Mîndrescu (2019).

The strong correlation between mean temperature and the ET_c was verified at the spatial and temporal distributions in Varanasi district. The northern part of the study area appears with higher mean temperatures (> 25.7°C), and the seasonal and annual ET_c maps indicate higher values in the north sides, too. For these findings, a contribution of crops' distribution can be seen, which occupies a large area of Varanasi district. From the analysis of temperature, precipitation and the ET_0 variables, the absolute changes between 1941 and 1970 were significant for the precipitation (a decrease by 100 mm) and ET_0 (a decrease by 65 mm), while for the future period, the temperature rise plays a key role in the variation of the annual and seasonal ET_c. However, the spatial distribution of temperature and precipitation in Varanasi district indicates that the northern area is drier and the southern area wetter.

The present survey indicates that the most important factor for water resources in Varanasi district is represented by the amount of precipitation. The analysis proves that the slight decrease in the mean air temperature was recorded between the 1950s and the 1980s, and a consistent decrease in the precipitation was recorded in the same periods of analysis in the Varanasi area. Owing to this, the seasonal and annual ET_c, but also the AET_c, values decreased slightly between these two periods. The major impact came from the decreasing precipitation, which further influenced the water availability in the study area directly.

Another important parameter, which indicates the aridization of Varanasi district, is De Martonne's aridity index. It denoted humid climate during the 1950s and both humid and sub-humid climates during the 1980s. From the inference of the two parameters (water availability and De Martonne's aridity index), the climate change effect was assessed at the spatial scale.

Čenčur Curk *et al.* (2014) show that the ET_0 is around 1,000 mm for Southeast Europe during the period 1991–2050, while Cheval *et al.* (2017) give an ET_0 up to 1,150 mm in Southeast Europe during the current century. The present results are not so distant compared with the previous studies from Europe, considering that Varanasi district is situated at lower latitudes and the regional climate conditions are showing the intense aridity of the area. The methodology applied in the present study is quite simple and easy to adapt to other study areas; for these reasons the authors agree with the difference of the results between Northern India and Southern Europe.

A few studies have tried to designate the main characteristics of future climate change scenarios and development pathways at the global scale (Elliott *et al.*, 2014; Schewe *et al.*, 2014). In the study area, the maximum area under Bundelkhand region (the southwestern part of Uttar Pradesh) has come under a drought-prone area where both surface and ground water conditions are continuously depleting.

The present study is not without its limitations. For the calculations of ET_c, the standard K_c values were used instead of field data measurement owing to the lack of historical data. Future investigations could be improved by lysimeter or pan measurements in each specific land cover type, water gauge measurements and hydrographs analysis in real time. Considering that the present study was focused on the long-term period, the standard K_c, empirical calculations and geographical information system (GIS) technology were assumed to fit better with the aim of the study. Water demand in the urban areas and the human factor were not considered in the present study owing to uncertainty in the data for the entire period. However, the main focus of the study was on the climate change effect, which is a more important factor regarding water resources. In addition, the spatial–temporal method applied here through the inference matrix offers good results at the district scale and may be useful for making preliminary decisions regarding climate change and water management.

6 | CONCLUSIONS

The climate change effect on water resources in Varanasi district of India was determined over the period 1941–2000 at the spatial scale. Calculations of seasonal and annual crop evapotranspiration (ET_c), including land cover data, together with actual crop evapotranspiration (AET_c) were computed based on historical climate records and land cover data for the area. Even though the annual ET_c and AET_c decreased slightly between the 1950s and 1980s, precipitation and water availability decreased in the 1980s, indicating a negative impact at the spatial scale. In addition, the Mann and Kendall test indicates a negative trend for all stations in the study area. A positive trend was found for mean annual temperature at major stations. The climate indices (Lang's rain factor and De Martonne's aridity index) denoted lower values for both indices for the recent period (1980s), which suggests that the climate of Varanasi district has a general tendency of aridization.

In order to assess the climate change effect on water resources, the water availability and De Martonne's aridity index were inserted into a 5×5 matrix. Through this matrix, five classes of this effect were determined between the two analysed periods in Varanasi district. The high and very high effect were depicted in the agricultural areas, mainly in the entire territory, while the medium and low effect were depicted in the constructed areas, artificial areas and wetlands.

Based on the present study, the agricultural and water management plans could be drawn by considering the more affected areas. The irrigation strategies and protection zones for water conservation could be delineated in the base of original maps, which represent important tools for the urban and rural planning of the study area.

Moreover, the maps used in the present study complete the spatial research gaps for Varanasi district with respect to climate and hydrology. Future work may be designated to the groundwater vulnerability calculation at the spatial scale, considering both climate and land cover factors.

ORCID

Mărgărit-Mircea Nistor https://orcid.org/0000-0001-9644-5853
Vikas Dugesar https://orcid.org/0000-0002-5937-2795
Virendra Kumar Kumra https://orcid.org/0000-0002-0275-491X

REFERENCES

Allen, R.G. (2000) Using the FAO-56 dual crop coefficient method over an irrigated region as part of an evapotranspiration intercomparison study. *Journal of Hydrology*, 229, 27–41.

Allen, R.G., Pereira, L.S., Raes, D. and Smith, M. (1998) *Crop Evapotranspiration: Guidelines for Computing Crop Water Requirements*. FAO Irrigation and Drainage Paper 56. FAO: Rome; pp. 300.

Bachu, S. and Adams, J.J. (2003) Sequestration of CO_2 in geological media in response to climate change: capacity of deep saline aquifers to sequester CO_2 in solution. *Energy Conversion and Management*, 44(20), 3151–3175.

Brouyère, S., Carabin, G. and Dassargues, A. (2004) Climate change impacts on groundwater resources: modelled deficits in a chalky aquifer, Geer basin, Belgium. *Hydrogeology Journal*, 12 (2), 1–33.

Budyko, M.I. (1974) *Climate and Life*. New York, NY: Academic Press, p. 508.

Čenčur Curk, B., Cheval, S., Vrhovnik, P., Verbovšek, T., Herrnegger, M., Nachtnebel, H.P., Marjanović, P., Siegel, H., Gerhardt, E., Hochbichler, E., Koeck, R., Kuschnig, G., Senoner, T., Wesemann, J., Hochleitner, M., Žvab Rožič, P., Brenčič, M., Zupančič, N., Bračič Železnik, B., Perger, L., Tahy, A., Tornay, E.B., Simonffy, Z., Bogardi, I., Crăciunescu, A., Bilea, I.C., Vică, P., Onuţ{t\hskip-0.7ex\char "B8}u, I., Panaitescu, C., Constandache, C., Bilanici, A., Dumitrescu, A., Baciu, M., Breza, T., Marin, L., Draghici, C., Stoica, C., Bobeva, A., Trichkov, L., Pandeva, D., Spiridonov, V., Ilcheva, I., Nikolova, K., Balabanova, S., Soupilas, A., Thomas, S., Zambetoglou, K., Papatolios, K., Michailidis, S., Michalopoloy, C., Vafeiadis, M., Marcaccio, M., Errigo, D., Ferri, D., Zinoni, F., Corsini, A., Ronchetti, F., Nistor, M.M., Borgatti, L., Cervi, F., Petronici, F., Dimkić, D., Matić, B., Pejović, D., Lukić, V., Stefanović, M., Durić, D., Marjanović, M., Milovanović, M., Boreli-Zdravković, D., Mitrović, G., Milenković, N., Stevanović, Z. and Milanović, S. (2014) *CC-WARE Mitigating Vulnerability of Water Resources under Climate Change*. WP3—Vulnerability of Water Resources in SEE, Report Version 5. Available at: http://www.ccware.eu/output-documentation/output-wp3.html. [Accessed 15th May 2017].

Cervi, F. and Nistor, M.M. (2018) High resolution of water availability for Emilia-Romagna region over 1961–2015. *Advances in Meteorology*, 2018, 1–13. https://doi.org/10.1155/2018/2489758.

Chattopadhyay, N. and Hulme, M. (1997) Evaporation and potential evapotranspiration in India under conditions of recent and future climate change. *Agricultural and Forest Meteorology*, 87 (1), 55–73.

Cheval, S., Baciu, M., Dumitrescu, A., Breza, T., Legates, D.R. and Chendeş, V. (2011) Climatologic adjustments to monthly precipitation in Romania. *International Journal of Climatology*, 31, 704–714.

Cheval, S., Dumitrescu, A. and Birsan, M.V. (2017) Variability of the aridity in the South-Eastern Europe over 1961–2050. *Catena*, 151, 74–86.

De Martonne, E. (1925) *Traité Géographie. Physique: 3 tomes*. Paris: Max leclcrc and H. Bourrclier, proprietors of Librairic Armard Colin (in French).

De Martonne, E. (1926) A new climatological function: the aridity index. *La Météorologie*, 2, 449–458 (in French).

Deniz, A., Toros, H. and Incecik, S. (2011) Spatial variations of climate indices in Turkey. *International Journal of Climatology*, 31, 394–403.

Dezsi, Ş., Mîndrescu, M., Petrea, D., Rai, K.P., Hamann, A. and Nistor, M.M. (2018) High-resolution projections of evapotranspiration and water availability for Europe under climate change. *International Journal of Climatology*, 38, 3832–3841.

Elliott, J., Deryng, D., Müller, C., Frieler, K., Konzmann, M., Gerten, D., Glotter, M., Flörke, M., Wada, Y., Best, N., Eisner, S., Fekete, B.M., Folberth, C., Foster, I., Gosling, S.N., Haddeland, I., Khabarov, N., Ludwing, F., Masaki, Y., Olin, S., Rosenzweig, C., Ruane, A.C., Satoh, Y., Schmid, E., Stacke, T., Tang, Q. and Wisser, D. (2014) Constraints and potentials of future irrigation water availability on agricultural production under climate change. *Proceedings of the National Academy of Sciences*, 111(9), 3239–3244. https://doi.org/10.1073/pnas.1222474110.

Espadafor, M., Lorite, I.J., Gavilán, P. and Berengena, J. (2011) An analysis of the tendency of reference evapotranspiration estimates and other climate variables during the last 45 years in Southern Spain. *Agricultural Water Management*, 98(6), 1045–1061.

Frich, P., Alexander, L.V., Della-Marta, P., Gleason, B., Haylock, M., Tank Klein, A.M.G. and Peterson, T. (2002) Observed coherent changes in climatic extremes during the second half of the twentieth century. *Climate Research*, 19(3), 193–212.

Fu, J.Y., Jiang, D. and Huang, Y.H. (2014) 1 km grid population dataset of China (2005, 2010) (Supplement). *Acta Geographica Sinica*, 69, 136–139. https://doi.org/10.3974/geodb.2014.01.06.V1.

Gerrits, A.M.J., Savenije, H.H.G., Veling, E.J.M. and Pfister, L. (2009) Analytical derivation of the Budyko curve based on rainfall characteristics and a simple evaporation model. *Water Resources Research*, 45(4), 1–15. https://doi.org/10.1029/2008WR007308.

Gilbert, R.O. (1987) *Statistical Methods for Environmental Pollution Monitoring*. New York, NY: Van Nostrand Reinhold.

Grimmond, C.S.B. and Oke, T.R. (1999) Evapotranspiration rates in urban areas, Impacts of Urban Growth on SurfaceWater and Groundwater Quality. *Proceedings of IUGG 99 Symposium HSS*, Birmingham, July 1999, pp. 235–243.

Hamed, K.H. (2008) Trend detection in hydrologic data: the Mann–Kendall trend test under the scaling hypothesis. *Journal of Hydrology*, 349, 350–363.

IPCC. (2013) Summary for policymakers. In: Stocker, T.F., Qin, D., Plattner, G.-K., Tignor, M., Allen, S.K., Boschung, J., Nauels, A., Xia, Y., Bex, V. and Midgley, P.M. (Eds.) *Climate Change 2013: The Physical Science Basis. Contribution of Working Group I to the Fifth Assessment Report of the Intergovernmental Panel on Climate Change*. Cambridge and New York, NY: Cambridge University Press, p. 1308.

Jiménez Cisneros, B.E., Oki, T., Arnell, N.W., Benito, G., Cogley, J. G., Döll, P., Jiang, T. and Mwakalila, S.S. (2014) Freshwater resources. In: Field, C.B., Barros, V.R., Dokken, D.J., Mach, K. J., Mastrandrea, M.D., Bilir, T.E., Chatterjee, M., Ebi, K.L., Estrada, Y.O., Genova, R.C., Girma, B., Kissel, E.S., Levy, A.N., MacCracken, S., Mastrandrea, P.R. and White, L.L. (Eds.) *Climate Change 2014: Impacts, Adaptation, and Vulnerability. Part A: Global and Sectoral Aspects. Contribution of Working Group II to the Fifth Assessment Report of the Intergovernmental Panel on Climate Change*. Cambridge, and New York, NY: Cambridge University Press, pp. 229–269.

Kendall, M.G. (1975) *Rank Correlation Methods*, 4th edition. London: Charles Griffin.

Kottek, M., Grieser, J., Beck, C., Rudolf, B. and Rubel, F. (2006) World Map of the Koppen–Geiger climate classification updated. *Meteorologische Zeitschrift*, 15(3), 259–263.

Lang, R. (1915) Versuch einer exakten Klassifikation der Boden in klimatischer und geologischer Hinsicht. *Internationale Mitteilungen für Bodenkunde*, 5, 312.

Loáiciga, H.A., Maidment, D. and Valdes, J.B. (2000) Climate change impacts in a regional karst aquifer. *Journal of Hydrology*, 227(1–4), 173–194.

Meinshausen, M., Meinshausen, N., Hare, W., Raper, S.C.B., Frieler, K., Knutti, R. and Allen, M.R. (2009) Greenhouse-gas emission targets for limiting global warming to 2°C. *Nature*, 458(7242), 1158–1162.

Moreau, R.E. (1938) Climatic classification from the standpoint of east African biology. *Journal of Ecology*, 26(2), 467–496.

Nistor, M.M. (2019) Groundwater vulnerability in Europe under climate change. *Quaternary International*. https://doi.org/10.1016/j.quaint.2019.04.012.

Nistor, M.M. and Mîndrescu, M. (2019) Climate change effect on groundwater resources in Emilia-Romagna region: an improved assessment through NISTOR-CEGW method. *Quaternary International*, 504, 214–228.

Nistor, M.M., Dezsi, S., Cheval, S. and Baciu, M. (2016) Climate change effects on groundwater resources: a new assessment method through climate indices and effective precipitation in Beliş district, Western Carpathians. *Meteorological Applications*, 23, 554–561.

Nistor, M.M., Man, T.C., Benzaghta, M.A., Nedumpallile Vasu, N., Dezsi, Ş. and Kizza, R. (2018) Land cover and temperature implications for the seasonal evapotranspiration in Europe. *Geographia Technica*, 13(1), 85–108.

Nistor, M.M., and Porumb-Ghiurco, G.C. (2015) How to compute the land cover evapotranspiration at regional scale? A spatial approach of Emilia-Romagna region. *GEOREVIEW Scientific Annals of Stefan cel Mare University of Suceava, Geography Series*, 25(1), 38–54.

Palumbo, A.D., Vitale, D., Campi, P. and Mastrorilli, M. (2011) Time trend in reference evapotranspiration: analysis of a long series of agrometeorological measurements in southern Italy. *Irrigation and Drainage Systems*, 25(4), 395–411.

Papaioannou, G., Kitsara, G. and Athanasatos, S. (2011) Impact of global dimming and brightening on reference evapotranspiration in Greece. *Journal of Geophysical Research Atmospheres*, 116(9), 1–13. https://doi.org/10.1029/2010JD015525.

Parry, M.L., Rosenzweig, C., Iglesias, A., Livermore, M. and Fischer, G. (2004) Effects of climate change on global food production under SRES emissions and socio-economic scenarios. *Global Environmental Change*, 14(1), 53–67.

Prăvălie, R. (2014) Analysis of temperature, precipitation and potential evapotranspiration trends in southern Oltenia in the context of climate change. *Geographia Technica*, 9(2), 68–84.

Prăvălie, R., Sîrodoev, I. and Peptenatu, D. (2014) Detecting climate change effects on forest ecosystems in Southwestern Romania using Landsat TM NDVI data. *Journal of Geographical Sciences*, 24(5), 815–832.

Quan, C., Han, S., Utescher, T., Zhang, C. and Liu (Christopher), Y. S. (2013) Validation of temperature–precipitation based aridity index: Paleoclimatic implications. *Palaeogeography, Palaeoclimatology, Palaeoecology*, 386, 86–95.

Quirk, T. (2012) Did the global temperature trend change at the end of the 1990s? *Asia-Pacific Journal of Atmospheric Sciences*, 48(4), 339–344.

Rai, P.K. and Mohan, K. (2014) Remote sensing data & GIS for flood risk zonation mapping in Varanasi District. *Forum Geographic Journal*, 13(1), 25–33. https://doi.org/10.5775/fg.2067-4635.2014.041.i.

Rai, P.K. and Nathawat, M.S. (2017) *Geoinformatics in Health Facility Analysis*. Cham, Switzerland: Springer. DOI: https://doi.org/10.1007/978-3-319-44624-0

Roy, P.S., Roy, A., Joshi, P.K., Kale, M.P., Srivastava, V.K., Srivastava, S.K. and Kushwaha, D. (2015) Development of decadal (1985–1995–2005) land use and land cover database for India. *Remote Sensing*, 7(3), 2401–2430.

Schewe, J., Heike, J., Gerten, D., Haddeland, I., Arnell, N.W., Clark, D.B., Dankers, R., Eisner, S., Fekete, B.M., Colón González, F.J., Gosling, S.N., Kim, H., Liu, X., Masaki, Y., Portmann, F.T., Satoh, Y., Stacke, T., Tang, Q., Wada, Y., Wisser, D., Albrecht, T., Frieler, K., Piontek, F., Warszawski, L. and Kabat, P. (2014) Multimodel assessment of water scarcity under climate change. *Proceedings of the National Academy of Sciences*, 111, 3245–3250.

Shan, N., Shi, Z., Yang, X., Gao, J. and Cai, D. (2015) Spatiotemporal trends of reference evapotranspiration and its driving factors in the Beijing–Tianjin Sand Source Control Project Region, China. *Agricultural and Forest Meteorology*, 200, 322–333.

Shaver, G.R., Canadell, J., Chapin, F.S., III, Gurevitch, J., Harte, J., Henry, G., Ineson, P., Jonasson, S., Melillo, J., Pitelka, L. and Rustad, L. (2000) Global warming and terrestrial ecosystems: a conceptual framework for analysis. *Bioscience*, 50(10), 871–882.

Tabari, H., Marofi, S., Aeini, A., Talaee, P.H. and Mohammadi, K. (2011) Trend analysis of reference evapotranspiration in the western half of Iran. *Agricultural and Forest Meteorology*, 151 (2), 128–136.

Thornthwaite, W. (1948) An approach toward a rational classification of climate. *American Geographical Society*, 38(1), 55–94.

Wang, K. and Dickinson, R.E. (2012) A review of global terrestrial evapotranspiration: observation. *Reviews of Geophysics*, 50, RG2005, 1–54. https://doi.org/10.1029/2011RG000373.1.

Watson, R.T. (2001) Climate Change 2001: Synthesis Report. A Contribution of Working Groups I, II, and III to the Third Assessment Report of the Integovernmental Panel on Climate Change.

Yu, P.S., Yang, T.C. and Chou, C.C. (2002) Effects of climate change on evapotranspiration paddy fields in southern Taiwan. *Climatic Change*, 54(1–2), 165–179.

Zambakas, J. (1992) *General Climatology*. Athens: Department of Geology, National and Kapodistrian University of Athens (in Greek).

Zhao, L., Xia, J., Xu, C., Wang, Z., Sobkowiak, L. and Long, C. (2013) Evapotranspiration estimation methods in hydrological models. *Journal of Geographical Sciences*, 23(2), 359–369.

Zuo, D., Xu, Z., Yang, H. and Liu, X. (2012) Spatiotemporal variations and abrupt changes of potential evapotranspiration and its sensitivity to key meteorological variables in the Wei River basin, China. *Hydrological Processes*, 26(8), 1149–1160.

SUPPORTING INFORMATION

Additional supporting information may be found online in the Supporting Information section at the end of this article.

How to cite this article: Nistor M-M, Rai PK, Dugesar V, *et al.* Climate change effect on water resources in Varanasi district, India. *Meteorol Appl*. 2020;27:e1863. https://doi.org/10.1002/met.1863